A Journal of the Gesellschaft Deutscher Chemiker
Angewandte Chemie
International Edition
www.angewandte.org

Title: Electrochemical Reduction of CO2 to CH3OH on hierarchical Pd/SnO2 nanosheets with abundant Pd-O-Sn interfaces

Authors: Wuyong Zhang, Qing Qin, Lei Dai, Ruixuan Qin, Xiaojing Zhao, Xumao Chen, Daohui Ou, Tracy T Chuong, Binghui Wu, and Nanfeng Zheng

To be cited as: *Angew. Chem. Int. Ed.* 10.1002/anie.201804142
Angew. Chem. 10.1002/ange.201804142

Link to VoR: http://dx.doi.org/10.1002/anie.201804142
http://dx.doi.org/10.1002/ange.201804142

WILEY-VCH

Electrochemical Reduction of CO_2 to CH_3OH on hierarchical Pd/SnO_2 nanosheets with abundant Pd-O-Sn interfaces

Wuyong Zhang, Qing Qin, Lei Dai, Ruixuan Qin, Xiaojing Zhao, Xumao Chen, Daohui Ou, Jie Chen,Tracy T Chuong, Binghui Wu* and Nanfeng Zheng*

Abstract: Electrochemical conversion of CO_2 into fuels using electricity generated from renewable sources helps to create an artificial carbon cycle. However, the low efficiency and poor stability hinder the practical use of most conventional electrocatalysts. In this work, a 2D hierarchical Pd/SnO_2 structure, ultrathin Pd nanosheets partially capped by SnO_2 nanoparticles, is designed to enable multi-electron transfer for selective electroreduction of CO_2 into CH_3OH. Such a structure design not only enhances the adsorption of CO_2 on SnO_2, but also weakens the binding strength of CO on Pd due to the as-built Pd-O-Sn interfaces, which is demonstrated to be critical to improve the electrocatalytic selectivity and stability of Pd catalysts. This work provides a new strategy to improve electrochemical performance of metal-based catalysts by creating metal-oxide interfaces for selective electroreduction of CO_2.

Transferring carbon dioxide (CO_2) to useful carbon-based fuels through electrochemistry using renewable electricity is an attractive way to alleviate the environment and energy crisis.[1] Over the past few decades, numerous catalysts have been developed and applied for electrochemical CO_2 reduction reaction (CO_2RR). Early work mostly focused on bulk metal catalysts,[2] which usually suffered from poor activity with low current density, poor selectivity with multiple products, and depressed stability during electrocatalysis. To tackle these problems, a series of nanostructured catalysts including metal, alloy, metal-oxides and metal chalcogenides have been developed to replace traditional bulk metal catalysts.[3] Among these nanocatalysts, palladium-based nanomaterials have shown great potential in CO_2RR due to their high mass activity.[4] When pure Pd nanocatalysts are used, the selectivity of products are often regulated by controlling the size of Pd nanoparticles (NPs) or the reduction potentials.[5] As for alloyed-Pd catalysts, the proper ratio of second metal to Pd is critical to obtain a high-selectivity product.[6] Nevertheless, so far majority of Pd-based nanomaterials just produce CO or $HCOO^-$ through $2e^-$ transfer in CO_2RR. Multi-electron reduction to obtain value-added products such as methanol has been rarely reported.[7]

Previous studies have demonstrated that CO intermediate is usually involved in multi-electron transfer during CO_2RR.[1a] Considering that Pd has high chemical affinity to CO and is thus easily poisoned by it,[8] the manipulation of both adsorption and activation of CO is crucial in the design of new Pd-based nanocatalysts to realize the production of value-added chemicals beyond $2e^-$ process. We now report in this work a two-dimensional (2D) hierarchical Pd/SnO_2 structure to meet such a demand on balancing CO adsorption and activation. 2D ultrathin Pd nanosheets (Pd NSs) with thickness of several atomic layers and thus large surface area[9] were chosen to provide abundant active sites for electrocatalysis.[10] The surface of Pd NSs were modified by depositing fine SnO_2 NPs, another widely-studied CO_2RR catalyst,[11] to form the hierarchical structure.[12] The partial capping of Pd NSs with SnO_2 helped to enhance the adsorption of CO_2 but weaken the CO binding on Pd. The as-built Pd-O-Sn interfaces was demonstrated to play a key role in electro-reduction of CO_2 to CH_3OH via a multi-electron transfer process.

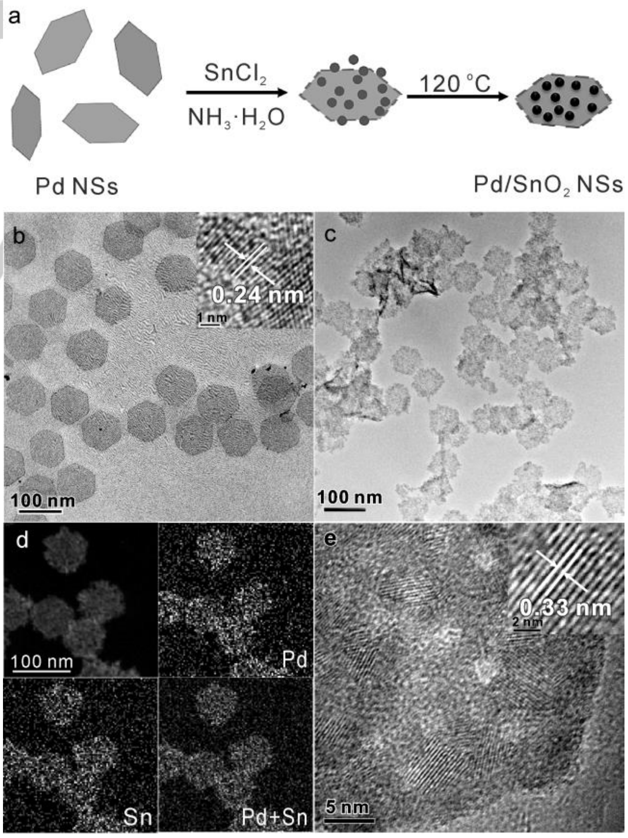

Figure 1. Structure characterization of Pd and hierarchical Pd/SnO_2 NSs. (a) Illustration for the synthesis of Pd/SnO_2 NSs. (b) TEM image of Pd NS seeds. (c) TEM image, (d) HAADF-STEM and EDX mapping, and (e) HRTEM images of Pd/SnO_2 NSs (Pd:Sn=1:1). Insets of b and e are corresponding HRTEM images showing interplanar lattice fringe spacing.

---

[*] W. Zhang, Q. Qin, Dr. L. Dai, R. Qin, Dr. X. Zhao, X. Chen, Dr. J. Chen, Prof. N. Zheng
State Key Laboratory for Physical Chemistry of Solid Surfaces, Collaborative Innovation Center of Chemistry for Energy Materials, National & Local Joint Engineering Research Center of Preparation Technology of Nanomaterials, College of Chemistry and Chemical Engineering, Xiamen University, Xiamen 361005 (China)
E-mail: nfzheng@xmu.edu.cn
D. Ou, Dr. T. T Chuong, Prof. B. Wu
Pen-Tung Sah Institute of Micro-Nano Science and Technology, Xiamen University, Xiamen 361005 (China)
E-mail: binghuiwu@xmu.edu.cn

Supporting information for this article is given via a link at the end of the document.

10.1002/anie.201804142

Partial capping of Pd NSs with SnO_2 NPs (denoted as Pd/SnO_2 NSs) was carried out using the precedure illustrated in Figure 1a (details in Supporting Information). Pd NS seeds were first dispersed in ethanol and water by adequate sonication in a round-bottom flask. $SnCl_2 \cdot 2H_2O$ was then added into the above mixture, followed by dropwise addition of $NH_3 \cdot H_2O$ under stirring. The black product was obtained after refluxing at 120 °C. The microstructure of as-prepared Pd/SnO_2 NSs was studied by transmission electron microscopy (TEM). As shown in Figure 1b-c, while surface roughness was observed, the structure and dimension of the Pd NSs remained unchanged after the deposition of SnO_2 NPs. Low magnification TEM images also showed that the product was uniform and free of unattached SnO_2 NPs (Figure S1). The attachment of these Pd/SnO_2 NSs on carbon nanotubes allowed the direct measurement of their overall thickness by TEM which is 4-6 nm, consistent with atomic force microscopy results (Figure S2). As verified by high-angle annular dark field-scanning transmission electron microscopy (HAADF-STEM) image and energy-dispersive X-ray (EDX) mapping (Figure 1d and S3), SnO_2 NPs are well-dispersed on each Pd NS. It should be noted that the surface of Pd NSs capped by SnO_2 is still partially exposed. An obvious CO stripping peak was observed on Pd/SnO_2 NSs although the intensity was lower than that of uncapped Pd NSs (Fig S4). The EDX analysis revealed that the Pd:Sn atomic ratio of Pd/SnO_2 NSs is 0.52:0.48 (Figure S5), which was further confirmed by the inductively coupled plasma mass spectroscopy (ICP-MS) result (0.54:0.46). The X-ray diffraction (XRD) pattern of Pd/SnO_2 NSs (Figure S6) is clearly indexed to fcc Pd (JCPDS#46-1043) and rutile SnO_2 (JCPDS#41-1445). The size of SnO_2 NPs analyzed by XRD is about 3-5 nm, consistent with the high-resolution TEM analysis (Figure 1e). As shown in Figure 1e, the single-crystalline nature of SnO_2 NPs with interplanar lattice fringe spacing of 0.33 nm, corresponding to the d-spacing of (110) plane of rutile SnO_2, was clearly observed.

In view of the unique microstructure of Pd/SnO_2 NSs, we conducted CO_2RR to investigate whether the as-fabricated Pd-SnO_2 interfaces would influence the catalysis of Pd. The Pd/SnO_2 NSs were loaded onto carbon paper to serve as a working electrode. Linear sweep voltammetry (LSV) test was performed in a H-cell with CO_2-saturated 0.1 M $NaHCO_3$ solution (pH=6.8). Poor electrochemical activity was found on both isolated Pd NSs and SnO_2 NPs (Figure S7). By contrast, Pd/SnO_2 NSs showed a remarkable enhancement of CO_2 reduction. As illustrated in Figure 2a, the Pd/SnO_2 NSs displayed a current density of -1.45 mA cm^{-2} at -0.24 V versus the reversible hydrogen electrode (RHE), significantly higher than those of Pd NSs and SnO_2 NPs. To identify the CO_2 reduction product, gas chromatography and ^{1}H NMR spectroscopy (Figure S8) were performed to quantify the gaseous and liquid products, respectively. To our surprise, different from the situations on single Pd NSs and SnO_2 NPs, multi-electron transfer in CO_2RR took place on Pd/SnO_2 NSs to produce CH_3OH as a major product, along with hydrogen and formate (Figure S9). As shown in Figure 2b, a maximum faradaic efficiency (FE) of 54.8±2% for CH_3OH was achieved at -0.24 V versus RHE. Compared to other reported catalysts (Table S1), Pd/SnO_2 NSs showed a decent current density with an ideal FE and low overpotential. To verify that the modification of SnO_2 on Pd created new active sites for CO_2RR, the electrochemical active surface area (ECSA) was measured via double-layer capacitance test in 0.1 M $NaHCO_3$ solution saturated with CO_2. ECSA of Pd/SnO_2 NSs is much larger than those of Pd NSs and SnO_2 NPs (Figure 2c), clearly confirming the close correlation between active sites and strong interaction of Pd and SnO_2. Moreover, as indicated in the Nyquist plots (Figure S10), CO_2 molecules have a smaller interfacial charge-transfer resistance on Pd/SnO_2 NSs. As a result, electrons can transfer easily to adsorbed CO_2 for forming the intermediate.[3a] In order to confirm the necessity of strong interaction between Pd and SnO_2, we mixed SnO_2 NPs with Pd NSs physically to test CO_2RR performance of the mixture. No liquid product of $HCOO^-$ or CH_3OH upon the electrolysis was obtained (Figure S11). Besides activity, durability is another important measure of an excellent catalyst. Pd/SnO_2 NSs did not show obvious attenuation on the current densities in chronoamperometry test (Figure 2d), and held the high FE of 54% over 24 h to produce CH_3OH from the time-tracking ^{1}H NMR (Figure S12). Moreover, the Pd/SnO_2 catalyst also maintained their original morphology and crystalline structure after the 24-h electrolysis (Figure S13). In addition, Pd/SnO_2 NSs could transfer CO_2 to methanol with a similar performance in different electrolytes (Figure S14). All these results suggested that the modification of Pd with SnO_2 greatly enhanced the catalysis of Pd in CO_2RR.

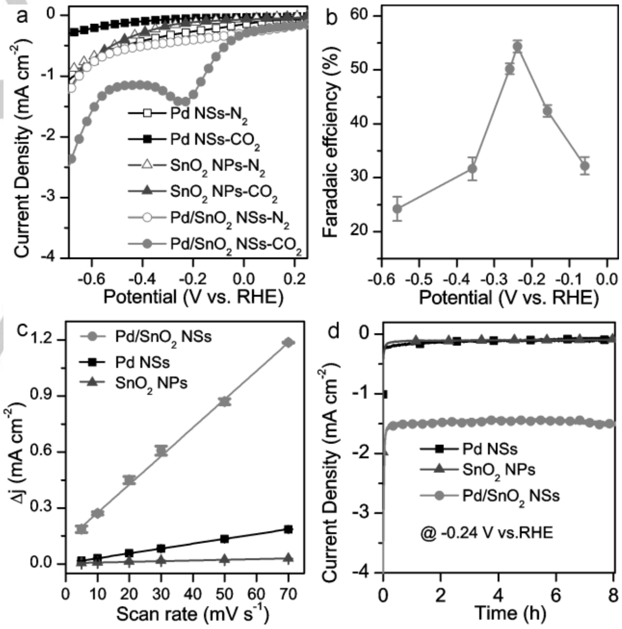

Figure 2. Electrochemical studies on Pd/SnO_2 NSs (Pd:Sn=1:1) in comparison with Pd NSs and SnO_2 NPs. (a) LSV curves in 0.1 M $NaHCO_3$ solution. (b) Faradaic efficiencies for CH_3OH at various applied potentials. (c) Charging current density differences plotted against scan rates. (d) Chronoamperometry results of different catalysts.

The combination of Pd and SnO_2 created an unexpected effect for the formation of CH_3OH, suggesting that the built-up Pd-SnO_2 interface should modulate the CO_2 and CO adsorption capacities of the catalyst. First of all, we found that the adsorption capacity of CO_2 on the Pd/SnO_2 NSs was significantly improved as compared to that of Pd NSs. As clearly revealed by the *in situ* diffuse reflectance infrared Fourier transform (DRIFT) spectroscopy data (Figure 3a and Figure S15), Pd/SnO_2 NSs displayed a much stronger absorption at 2,350 cm^{-1} that those on SnO_2 NPs and Pd NSs. The CO_2-TPD (temperature programmed desorption) measurements (Figure S16) also confirmed the excellent capacity of CO_2 adsorption on Pd/SnO_2 NSs, which is beneficial to CO_2RR. Secondly, Pd atoms on Pd/SnO_2 NSs are partially exposed. As clearly shown in the CO stripping (Figure 3b), SnO_2 NPs are unable to bind CO, but the Pd/SnO_2 NSs inherit the CO binding ability of Pd NSs. Since CO has been well-documented as an important intermediate in CO_2 electroreduction to CH_3OH, such a CO-binding capability of Pd/SnO_2 NSs made it is possible to further reduce CO during CO_2RR.[1a] More importantly, the modification of SnO_2 helped to weaken CO poisoning on Pd. Compared to that on Pd NSs, the CO stripping potential on Pd/SnO_2 NSs is slightly shifted towards a lower potential (Figure S17a). To further evaluated the effect of SnO_2, the coverage of SnO_2 on Pd/SnO_2 NSs was tuned by different Pd:Sn ratio in synthesis (Figure S18). Figure 3c shows the potential-dependent FEs of Pd/SnO_2 NSs with different Pd/Sn ratios. While the Pd/SnO_2 NSs with low ratio of SnO_2 (Pd:Sn=3 : 1) had H_2 as the major product, the increase of SnO_2 content on Pd NSs increased the FEs of $HCOO^-$ and CH_3OH. No matter what potential applied, the total FE of $HCOO^-$ and CH_3OH reached a maximum value when Pd:Sn ratio is 1:1. As confirmed by the CO stripping data (Figure S17), the increased content of SnO_2 reduced Pd exposure. It is thus reasonable to tune the Pd/Sn ratio in Pd/SnO_2 NSs for maximizing the FE of CH_3OH.

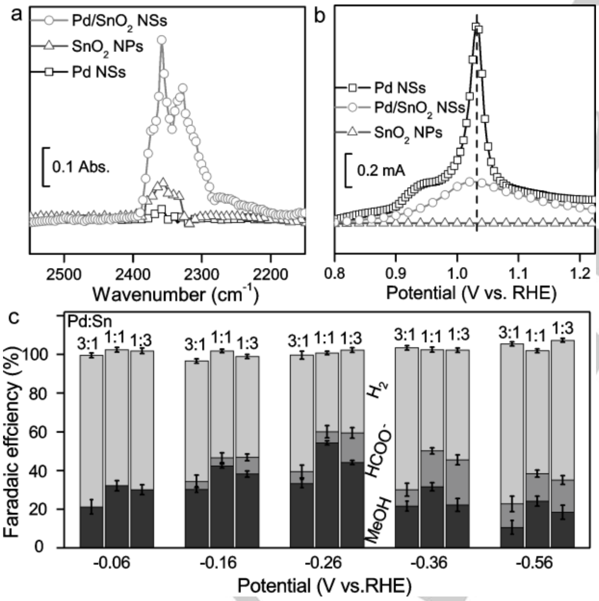

Figure 3. Adsorption of CO_2/CO and effects of Pd/Sn ratio on FEs. (a) *In situ* DRIFTS of CO_2 saturated adsorption. (b) CO stripping voltammetry. (c) Faradaic efficiencies for methanol, formate, and hydrogen at different voltages.

Considering that many metal-oxide interfaces have been reported to play important roles in electrocatalysis,[13] we proposed that the Pd-SnO_2 interface is crucial for the observed promotional effect in this work. We thus conducted X-ray absorption studies to evaluate the interface structure of Pd/SnO_2. As revealed by extend X-ray absorption fine structure (EXAFS) spectra (Figure 4a), there is one smaller peak of Pd/SnO_2 NSs at ~1.5 Å from the Pd-O contribution, and a peak at ~2.5 Å from the Pd-Pd contribution referring to the standard sample (Figure S19). Further EXAFS fitting analysis (Table S2) revealed that the coordination number (C.N.) of Pd-Pd in Pd/SnO_2 NSs is 4.5, much lower than that of 9 in Pd NSs, indicating the partial oxidation of Pd in Pd/SnO_2 NSs. The oxidation state of Pd in Pd/SnO_2 NSs was also confirmed by the white-line intensity in the X-ray near-edge structure (XANES) (Figure 4b), X-ray photoelectron spectroscopy (XPS) and Raman spectra. As shown in Figure S20, XPS peaks at 336.8 eV (Pd $3d_{5/2}$) and 342.4 eV (Pd $3d_{3/2}$) are assigned to Pd(II).[14] In the Raman spectra (Figure S21), the hump peak near 628 cm^{-1} happens to be the overlap of the A_{1g} vibration mode of SnO_2 at 635 cm^{-1} and B_{1g} vibration mode of PdO at 636 cm^{-1}.[15] As for Sn in Pd/SnO_2 NSs, the electronic structure is close to that of pure SnO_2 NPs from the EXAFS and XANES spectra (Figure S22 and S23), but has a lower coordination number than SnO_2 NPs (Table S3). In view of this, we speculated the formation process of Pd/SnO_2 NSs as that Sn(II) went through the hydrolysis and oxidation to Sn(IV) under the alkaline condition,[16] and Pd NSs acted as a support.[17] With the deposition of SnO_2, some surface Pd atoms on Pd NSs were inevitably oxidized to create Pd-O-Sn interfaces.

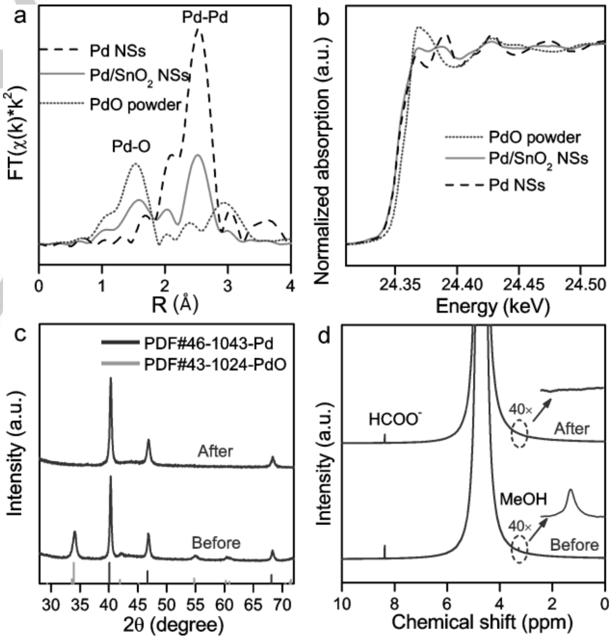

Figure 4. Evaluation of Pd-O interfaces in Pd/SnO_2 NSs (Pd:Sn=1:1). Pd K-edge (a) FT-EXAFS and (b) XANES spectra. (c) XRD patterns and (d) ^{1}HNMR spectra of liquid products before and after electrolysis of Pd/PdO catalyst.

After proving the presence of Pd-O-Sn interfaces in the Pd/SnO_2 NSs, we further explored the effect of the built the interfaces on CO_2RR. For comparison, we synthesized a Pd-PdO catalyst to simulate Pd/SnO_2 NSs by heating $Pd(OAc)_2$ in air. Multi-potential step electrolysis was conducted on the catalyst in 0.1 M $NaHCO_3$ solution under CO_2 atmosphere (Figure S24). Interestingly, there was a current fluctuation in the initial 2-hour electrolysis (Figure S24a), which was probably due to the reduction of PdO to Pd. Indeed, the XRD analysis (Figure 4c) revealed that the initial Pd-PdO was completely reduced and transferred to metallic Pd after the electrolysis. Meanwhile, both formate and CH_3OH were detected as electrolytic products in this process (Figure 4d). However, only formate was detected when the as-resulted pure Pd electrode was re-used for CO_2RR in fresh electrolyte. We thus speculate the Pd-oxide interface plays a catalytic role on CO_2 electroreduction to CH_3OH. As proposed in Figure S25, the electroreduction of CO_2 on Pd/SnO_2 NSs takes place with CO_2 first adsorbs on the surface of SnO_2 and reduces to $CO_2^{\bullet -}$.[3a] Then $CO_2^{\bullet -}$ gets further electrons and H^+ to form CO_{ads}.[3b] While competing with Pd(II) for electrons, the CO intermediate has priority to be further reduced to CH_3OH. The process is consistent with the mechanism for CO_2 electroreduction to CH_3OH as reported.[1a, 1b] Thinking about the possibility of $HCOO^-$ as an intermediate to get methanol,[1a] CO and $HCOO^-$ were individually used as starting materials and compared in similar electroreduction (Figure S26); NMR results showed that CO could be reduced to methanol but not $HCOO^-$, proving that the CO pathway was fit for Pd/SnO_2 NSs. To prove the general importance of Pd-O-Sn interfaces on CO_2RR, we also synthesized the Pd Black/SnO_2 via the similar $SnCl_2$ hydrolysis (Figure S27). The catalyst was found to be highly effective for the electroreduction CO_2 to CH_3OH (Figure S28) with a FE of 34%. The stability of Pd-O-Sn interfaces in Pd/SnO_2 NSs was also tested (Figure S29). After 8-h electrolysis with a high current density, the Pd-O-Sn interfaces still survived to give a relatively stable current. These results demonstrated that the strong interaction between Pd and SnO_2 and as the built-up Pd-O-Sn interfaces gave rise to the electrocatalytic selectivity and stability for the formation of CH_3OH.

In conclusion, we have built a hierarchical 2D material by partially capping Pd NSs with SnO_2 NPs for the electrochemical reduction of CO_2. Compared to single Pd NSs and SnO_2 NPs, the hierarchical Pd/SnO_2 NSs displayed a much better performance in the multi-electron transfer reduction of CO_2 into CH_3OH. The selectivity and long-term stability were readily optimized by tuning the coverage of SnO_2 on Pd NSs. The high selectivity toward CH_3OH are attributed to three factors: (1) Pd/SnO_2 NSs possess excellent adsorption capacity of CO_2; (2) partially exposed Pd on Pd/SnO_2 NSs adsorbs CO* intermediate for further electroreduction; (3) the existence of Pd-O-Sn interfaces assists further reduction of CO* intermediate to CH_3OH. Given current advances in the synthesis of hierarchical metal-oxide heterostructures, the proposed strategy may open up a new avenue to realized multi-electron transfer in CO_2RR.

Acknowledgements

The authors acknowledge support from the Ministry of Science and Technology of China (2017YFA0207302, 2015CB932300), the National Natural Science Foundation of China (21731005, 21420102001, 21333008, and 21721001), and the fundamental research funds for central universities (20720160080). We also acknowledge support from beamline BL14W1 (Shanghai Synchrotron Radiation Facility) for providing beam time.

Keywords: CO_2 reduction reaction (CO_2RR) • palladium • tin oxide • methanol • interface

[1] a) J. Albo, M. Alvarez-Guerra, P. Castaño, et al., *Green Chem.* **2015**, *17*, 2304-2324; b) X. Sun, Q. Zhu, X. Kang, et al., *Angew. Chem. Int. Ed.* **2016**, *55*, 6771-6775; c) M. Asadi, B. Kumar, A. Behranginia, et al., *Nat. Commun.* **2014**, *5*, 4470; d) S. Gao, X. Jiao, Z. Sun, et al., *Angew. Chem. Int. Ed.* **2016**, *55*, 698-702; e) K. P. Kuhl, T. Hatsukade, E. R. Cave, et al., *J. Am. Chem. Soc.* **2014**, *136*, 14107-14113; f) M. Asadi, K. Kim, C. Liu, et al., *Science* **2016**, *353*, 467-470; g) Y. Hori, H. Wakebe, T. Tsukamoto, et al., *Electrochim. Acta.* **1994**, *39*, 1833-1839.

[2] Y. Hori, *Modern Aspects of Electrochemistry*, Springer, **2008**.

[3] a) D. D. Zhu, J. L. Liu, S. Z. Qiao, *Adv. Mater.* **2016**, *28*, 3423-3452; b) L. Zhang, Z. J. Zhao, J. Gong, *Angew. Chem. Int. Ed.* **2017**, *56*, 11326-11353.

[4] a) A. Chen, C. Ostrom, *Chem. Rev.* **2015**, *115*, 11999-12044; b) C. Bianchini, P. K. Shen, *Chem. Rev.* **2009**, *109*, 4183-4206.

[5] a) D. Gao, H. Zhou, J. Wang, et al., *J. Am. Chem. Soc.* **2015**, *137*, 4288-4291; b) W. Sheng, S. Kattel, S. Yao, et al., *Energy Environ. Sci.* **2017**, *10*, 1180-1185.

[6] a) X. F. Bai, W. Chen, C. C. Zhao, et al., *Angew Chem Int Edit* **2017**, *56*, 12219-12223; b) S. Ma, M. Sadakiyo, M. Heima, et al., *J. Am. Chem. Soc.* **2017**, *139*, 47-50.

[7] R. Kortlever, I. Peters, C. Balemans, et al., *Chem. Commun.* **2016**, *52*, 10229-10232.

[8] D. Gao, H. Zhou, F. Cai, et al., *Nano Res.* **2017**, *10*, 2181-2191.

[9] X. Huang, S. Tang, X. Mu, et al., *Nat. Nanotechnol.* **2011**, *6*, 28-32.

[10] a) Y. Sun, S. Gao, F. Lei, et al., *Chem. Soc. Rev.* **2015**, *44*, 623-636; b) L. Dai, Q. Qin, X. Zhao, et al., *Sci. Adv.* **2017**; c) G. Fiori, F. Bonaccorso, G. Iannaccone, et al., *Nat. Nanotechnol.* **2014**, *9*, 768-779; d) J. Liu, C. Guo, A. Vasileff, et al., *Small Methods* **2017**, *1*, 1600006; e) S. Gao, Y. Lin, X. Jiao, et al., *Nature* **2016**, *529*, 68-71; f) Z. Sun, T. Ma, H. Tao, et al., *Chem* **2017**, *3*, 560-587; g) M. Chen, B. Wu, J. Yang, et al., *Adv. Mater.* **2012**, *24*, 862-879.

[11] a) H. Won da, C. H. Choi, J. Chung, et al., *ChemSusChem* **2015**, *8*, 3092-3098; b) F. Li, L. Chen, G. P. Knowles, et al., *Angew. Chem. Int. Ed.* **2017**, *56*, 505-509; c) F. Lei, W. Liu, Y. Sun, et al., *Nat. Commun.* **2016**, *7*, 12697; d) Q. Li, J. Fu, W. Zhu, et al., *J. Am. Chem. Soc.* **2017**, *139*, 4290-4293; e) Y. Chen, M. W. Kanan, *J. Am. Chem. Soc.* **2012**, *134*, 1986-1989.

[12] H. Wang, A. L. Rogach, *Chem. Mater.* **2014**, *26*, 123-133.

[13] a) D. Gao, Y. Zhang, Z. Zhou, et al., *J. Am. Chem. Soc.* **2017**, *139*, 5652-5655; b) W.-P. Zhou, S. Axnanda, M. G. White, et al., *J. Phys. Chem. C.* **2011**, *115*, 16467-16473; c) K. Mudiyanselage, S. D. Senanayake, L. Feria, et al., *Angew. Chem. Int. Ed.* **2013**, *52*, 5101-5105; d) X. Zheng, P. De Luna, F. P. García de Arquer, et al., *Joule* **2017**, *1*, 794-805.

[14] M. Brun, A. Berthet, J. C. Bertolini, *J. Electron. Spectrosc. Relat. Phenom.* **1999**, *104*, 55-60.

[15] a) Y. Zheng, T. Zhou, C. Zhang, et al., *Angew. Chem. Int. Ed.* **2016**, *55*, 3408-3413; b) A. Baylet, P. Marecot, D. Duprez, et al., *Phys. Chem. Chem. Phys.* **2011**, *13*, 4607-4613.

[16] H. K. Wang, A. L. Rogach, *Chem. Mater.* **2014**, *26*, 123-133.

[17] a) R. Liu, A. Sen, *J. Am. Chem. Soc.* **2012**, *134*, 17505-17512; b) B. H. Wu, D. Y. Liu, S. Mubeen, et al., *J. Am. Chem. Soc.* **2016**, *138*, 1114-1117.

COMMUNICATION

A 2D hierarchical Pd/SnO_2 structure, based on ultrathin Pd nanosheets partially capped by SnO_2 nanoparticles, was designed to enable multi-electron transfer for electroreduction of CO_2 to CH_3OH. The upgraded adsorption of CO_2 on the SnO_2 surface, proper binding of CO to Pd, and unique Pd-O-Sn interfaces were critical factors for the electrocatalytic selectivity and stability.

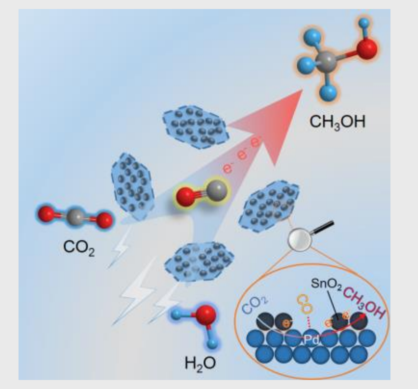

Wuyong Zhang, Qing Qin, , Lei Dai, Ruixuan Qin, Xiaojing Zhao, Xumao Chen, Daohui Ou, Jie Chen, Tracy T Chuong, Jie Chen, Binghui Wu and Nanfeng Zheng**

Page No. – Page No.

Electrochemical reduction of CO_2 to CH_3OH on hierarchical Pd/SnO_2 nanosheets with Abundant Pd-O-Sn interfaces